*Journal of Photoscience*, Vol. 3, No. 1, pp. 43–47, 1996
Printed in the Republic of Korea. 

ISSN 1225-8555/96


# Electronic Spectroscopy and Ligand Field Analysis of *Λ*-*fac*-Tris(L-alaninato)chromium(III)†

JONG-HA CHOI
Department of Chemistry, Andong National University, Andong 760-749, Korea

(*Received* 15 *January* 1996; *accepted* 21 *February* 1996)

**Abstract** — The 77 K emission and excitation, and room-temperature UV-visible spectra of *Λ*-*fac*-[Cr(L-ala)$_3$] (ala = alanine anion) have been measured. The ten electronic transitions due to spin-allowed and spin-forbidden are assigned. With the observed electronic transition energies, ligand field optimizations have been performed to determine the bonding properties of L-alanine anion toward chromium(III). The angular overlap model (AOM) parameters obtained indicate that it is electron-donating ligand which has values of $e_{\sigma O}$, $e_{\pi O}$, and $e_{\sigma N}$ slightly lower than those of glycine anion (gly). It seem that the decrease of the ligand field properties is due to steric effect of extra methyl group and inductive effect of adjacent carbonyl group.

## INTRODUCTION

The application of electronic spectroscopy to chromium(III) complexes with peptides and amino acids as ligands promises to provide a large amount of information concerning metal-protein interactions.[2,3] With the use of excitation spectroscopy the narrow intraconfigurational transitions due to the spin-forbidden in chromium(III) system can be located with a precision two orders of magnitude greater than the broad spin-allowed bands. The sharp line splittings are also very sensitive to the metal-ligand geometry.[4] Thus it is possible to obtain structural information from electronic spectroscopy without a full X-ray structure determination.[5]

Alanine differs from glycine by one methyl group. There are four possible geometric diastereomers of tris(L-alaninato)chromium(III) as shown in Figure 1. Among them the two facial isomers were only isolated, and their chemical properties were reported.[6] The circularly polarized luminescence and infrared spectra were also measured.[7,8] To date, however, there have been no reports on the ligand field properties of alanine anion toward any metal ion.

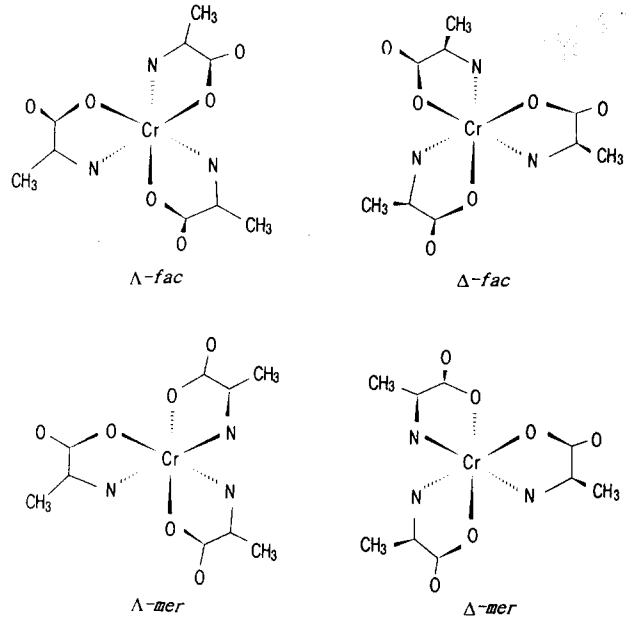


Figure 1. Theoretically possible geometric isomers of tris(L-alaninato)chromium(III).

In this study we have measured the 77 K emission and excitation, and room-temperature UV-visible spectra of *Λ*-*fac*-[Cr(L-ala)$_3$]. The ten electronic origins were assigned by analyzing the absorption and excitation spectra. Ligand field analysis of the observed electronic transitions was performed to determine the bonding properties for the coordinated oxygen and nitrogen atoms of L-alanine anion toward chromium(III).

†This is part 18 of the series *Electronic Structure and Chemical Reactivity of Transition Metal Complexes*. Reference 1 is regarded as part 17.

## MATERIALS AND METHODS

All chemicals were reagent grade quality and used without further purification. **Λ**-*fac*-Tris(L-alaninato) chromium(III) was prepared as described in the literature.[6] Tris(alaninato)chromium(III) is essentially insoluble in all solvents, and tend to decompose when left standing in contact with water. Therefore, recrystallization of the title complex was not possible, we had to get as pure a sample as possible on the first preparation of product.

The room-temperature absorption spectrum in aqueous solution was recorded with a Hewlett-Packard Model 8452A diode array spectrophotometer. The emission and excitation spectra were measured at 77 K on a Spex Fluorolog-2 spectrofluorometer as described previously.[9]

All optimizations and calculations for the ligand field parameterization were performed on an IBM mainframe computer. Some smaller computations and data manipulations were done on IBM compatible pentium microcomputer with an 16 MB main memory.

## RESULTS AND DISCUSSION

*Electronic Transitions.* The UV-visible absorption spectrum (solid line) of **Λ**-*fac*-[Cr(L-ala)$_3$] is represented in Figure 2.

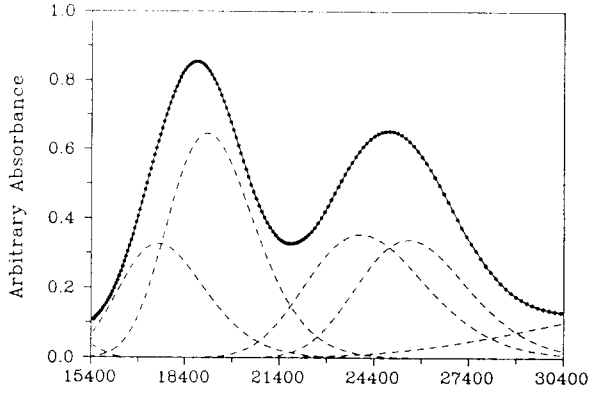


Figure 2. Deconvoluted absorption spectrum of **Λ**-*fac*-[Cr(L-ala)$_3$] in aqueous solution at room-temperature.

It exhibits two bands, one at 18730 cm$^{-1}$ ($\nu_1$) and the other at 24880 cm$^{-1}$ ($\nu_2$), corresponding to the $^4A_{2g} \rightarrow {}^4T_{2g}$ and $^4A_{2g} \rightarrow {}^4T_{1g}(O_h)$ transitions, respectively. The quartet bands have nearly symmetric profiles. In order to have some point of reference for the splittings of the two bands, we have fit the band profile to four Gaussian curves. A deconvolution procedure on the experimental band pattern yields maxima at 17760, 19230 and 24240, 25970 cm$^{-1}$ for the noncubic split levels of $^4T_{2g}$ and $^4T_{1g}$, respectively. We used these peak positions as the experimental transition energies. In fact, using just one Gaussian curve instead of two yields a least-squares error only four times that of the best fit (dashed line) shown in Figure 2.

An experimental problem lies with the difficulty in distinguish pure electronic components from the vibronic bands that also appear in the excitation spectrum. It is required that the vibrational intervals due to the electronic ground state are obtained by measuring emission spectrum with far-infrared spectral data. The 524 nm excited 77 K emission spectrum of **Λ**-*fac*-[Cr(L-ala)$_3$] is shown in Figure 3. The band positions relative to the lowest zero-phonon line, with corresponding infrared frequencies, are listed in Table 1. The emission spectrum was independent of the exciting wavelength within the first spin-allowed transition region.

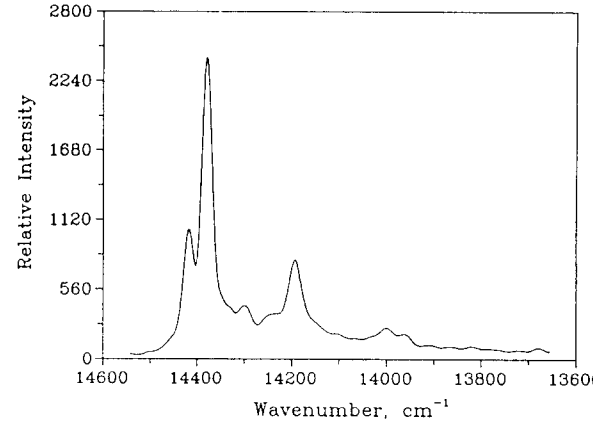


Figure 3. Emission spectrum of **Λ**-*fac*-[Cr(L-ala)$_3$] at 77 K.

Table 1. Vibrational intervals in the 77 K emission and 298 K infrared Spectra of **Λ**-*fac*-[Cr(L-ala)$_3$][a]

| Emission[b] | Infrared[c] | Assignment |
|---|---|---|
| -38 vs | | $R_2$ |
| 0 vs | | $R_1$ |
| 80 m | | Lattice vib. |
| 135 sh | | |
| 188 s | 175 s | δ(N-Cr-O) |
| 227 sh | 222 s, 235 sh | δ(N-Cr-N) |
| 272 w | 278 m | |
| 311 vw | 308 m | |
| 380 m | 386 s, 397 s | ν(Cr-O) |
| 417 m | 418 sh | ν(Cr-N) |
| 472 w | | ν(Cr-N) |
| 514 w | | |
| 560 w | 562 s | 188 + 380 |
| 595 w | | 188 + 417 |
| 624 vw | 625 m | |
| 702 w | 690 s | |

[a] Data in cm$^{-1}$. [b] Measured from zero-phonon line at 14380 cm$^{-1}$. [c] From ref. 8.

The most strong peak at 14380 cm$^{-1}$ is assigned as the zero-phonon line, $R_1$, because a corresponding strong peak is found at 14378 cm$^{-1}$ in the excitation spectrum. A well defined hot band at 14418 cm$^{-1}$ which may be assigned to the second component of the $^2E_g \rightarrow {}^4A_{2g}$ transition. The vibronic intervals occurring in the spectrum consist of several modes can be presumed to involve primarily ring torsion and angle-bending modes with frequencies below 311 cm$^{-1}$. The band at 472 cm$^{-1}$ can be assigned as a Cr-N stretching mode. The weak band at 417 cm$^{-1}$ in the emission spectrum have counterparts in the infrared spectrum, and can also be assigned as Cr-N stretching modes.[10]

The 77 K excitation spectrum is shown in Figure 4. It was recorded by monitoring a relatively strong vibronic peak in the emission spectrum. The spectrum obtained was independent of the vibronic peak used to monitor it. The peak positions and their assignments are tabulated in Table 2. The calculated frequencies in parentheses was obtained by using the vibrational modes $\nu_1 \sim \nu_7$ listed in Table 2.

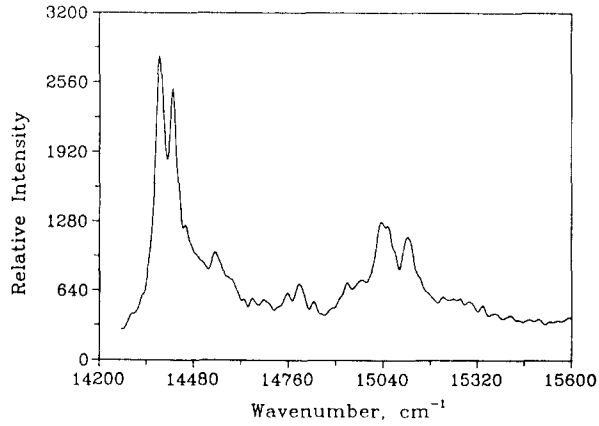


Figure 4. Excitation spectrum of $\Lambda$-*fac*-[Cr(L-ala)$_3$] at 77 K.

Two strong peaks at 14378 and 14418 cm$^{-1}$ in the excitation spectrum coincide with the luminescence spectrum are assigned to the two components ($R_1$ and $R_2$) of the $^2A_{2g} \rightarrow {}^2E_g$ transition. The lowest-energy zero-phonon line coincides within 2 cm$^{-1}$ with the emission origin. In general, it is not easy to locate positions of the other electronic components because the vibronic sidebands of the $^2E_g$ levels overlap with the lines of $^2T_{1g}$. However, the three components of the $^4A_{2g} \rightarrow {}^2T_{1g}$ electronic origin ($T_1$, $T_2$ and $T_3$) can be found with strong intensities 655, 680 and 728 cm$^{-1}$ from the lowest electronic line, $R_1$. Expanded portion of the spectral region and best-fit resolution are also shown in Figure 5. Vibronic satellites based on these origins also have similar frequencies and intensity

Table 2. Peak positions in the 77 *K* sharp line excitation spectrum of $\Lambda$-*fac*-[Cr(L-ala)$_3$][a]

| $\bar{\nu}_0$-14378 | Assignment | (Calcd)[b] | Vibronic frequencies | | Ground state frequencies[c] |
|---|---|---|---|---|---|
| 0 vs | $R_1$ | | $\nu_1$ | 80 | 79 |
| 40 vs | $R_2$ | | $\nu_2$ | 188 | 180 |
| 77 w | $R_1 + \nu_1$ | (79) | $\nu_3$ | 227 | 233 |
| 165 m | $R_1 + \nu_2$ | (180) | $\nu_4$ | 272 | 269 |
| 250 vw | $R_1 + \nu_1 + \nu_2$ | (259) | $\nu_5$ | 311 | 312 |
| 274 w | $R_2 + \nu_3$ | (273) | $\nu_6$ | 380 | 374 |
| 308 w | $R_2 + \nu_4$ | (309) | $\nu_7$ | 417 | 413 |
| 378 w | $R_1 + \nu_6$ | (374) | $\nu_8$ | 472 | 474 |
| 413 m | $R_2 + \nu_6$ | (414) | | | |
| 457 w | $R_1 + \nu_1 + \nu_6$ | (453) | | | |
| 554 w | $R_1 + \nu_2 + \nu_6$ | (554) | | | |
| 599 sh | $R_2 + \nu_2 + \nu_6$ | (594) | | | |
| 624 vw | $R_1 + 2\nu_5$ | (624) | | | |
| 655 s | $T_1$ | | | | |
| 680 s | $T_2$ | | | | |
| 698 m | $R_2 + \nu_2 + \nu_8$ | (694) | | | |
| 728 s | $T_3$ | | | | |
| 746 m | $R_1 + \nu_4 + \nu_8$ | (743) | | | |
| 769 w | $T_2 + \nu_1$ | (759) | | | |
| 838 vw | $T_1 + \nu_2$ | (835) | | | |
| 868 vw | $T_2 + \nu_2$ | (860) | | | |
| 889 vw | $T_1 + \nu_3$ | (888) | | | |
| 915 vw | $T_3 + \nu_2$ | (908) | | | |
| 957 w | $T_3 + \nu_3$ | (961) | | | |
| 995 vw | $T_2 + \nu_5$ | (992) | | | |
| 1040 w | $T_3 + \nu_5$ | (1040) | | | |
| 1064 vw | $T_1 + \nu_7$ | (1068) | | | |
| 1097 vw | $T_2 + \nu_7$ | (1093) | | | |
| 1126 w | $T_1 + \nu_8$ | (1129) | | | |
| 1157 vw | $T_2 + \nu_8$ | (1154) | | | |
| 1181 vw | $T_3 + \nu_1 + \nu_6$ | (1181) | | | |
| 1215 vw | $T_3 + \nu_1 + \nu_7$ | (1220) | | | |

[a] Data in cm$^{-1}$. [b] Values in parentheses represent the calculated frequencies based on the vibrational modes listed. [c] From the luminescence spectrum (Table 1).

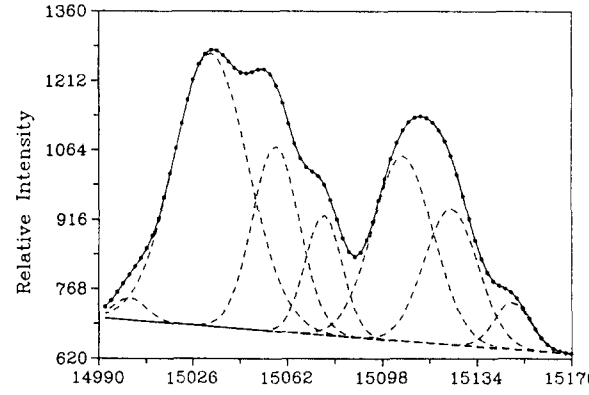


Figure 5. Expanded portion of the $^4A_{2g} \rightarrow {}^2T_{1g}$ electronic orgins and their resolved Gaussian components.

patterns to those of the $^2E_g$ components.

The higher energy $^4A_{2g} \rightarrow {}^2T_{2g}$ band was found at 20665 $cm^{-1}$ from the second derivative of the solution absorption spectrum shown with dashed line in Figure 6, but it could not be resolved into the separate components.

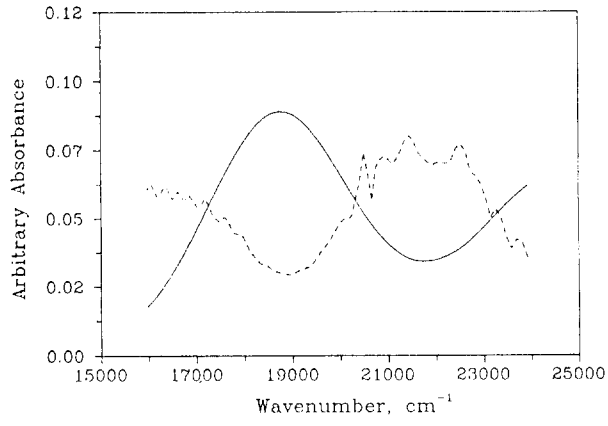


Figure 6. Absorption spectrum (solid line) and its second derivative spectrum (dashed line) of *Λ*-*fac*-[Cr(L-ala)$_3$] in aqueous solution.

*Ligand Field Calculations*. The ligand field potential matrix was generated for *Λ*-*fac*-[Cr(L-ala)$_3$] from the six coordinated nitrogen and oxygen atoms. The crystal structure of *Λ*-*fac*-[Cr(L-ala)$_3$] has not been known, we have adapted the positional parameters of coordinated atoms from the molecular geometry based on molecular mechanics calculation.[9] The coordinates were then rotated so as to maximize the projections of the six-coordinated atoms on the Cartesian axes centered on the chromium. The resulting Cartesian and spherical coordinates are shown in Table 3.

Table 3. Optimized Cartesian and spherical polar coordinates for ligating six atoms and adjacent carbonyl carbons in *Λ*-*fac*-[Cr(L-ala)$_3$][a]

| Atom | $x$ | $y$ | $z$ | $\theta$ | $\phi$ | $\psi$ |
|---|---|---|---|---|---|---|
| $O_1$ | -0.0206 | 0.1173 | 1.8378 | 3.71 | 99.96 | -14.88 |
| $O_2$ | 0.1334 | -1.8322 | 0.0526 | 88.36 | -85.84 | -87.09 |
| $O_3$ | 1.8448 | -0.0365 | -0.1614 | 95.00 | -178.87 | 6.96 |
| $N_1$ | -0.1295 | 0.0027 | -1.9227 | 176.15 | 178.81 | 0.00 |
| $N_2$ | 0.0321 | 1.9233 | 0.1593 | 85.27 | 89.04 | 0.00 |
| $N_3$ | 1.9176 | -0.1306 | -0.0454 | 91.35 | -3.90 | 0.00 |
| $C_1$ | 0.0688 | 1.2911 | 2.4922 | | | |
| $C_2$ | 1.3236 | -2.4567 | 0.1309 | | | |
| $C_3$ | -2.4519 | -0.1868 | -1.3513 | | | |

[a] Cartesian coordinates in Å, polar coordinates in degrees.

Angular overlap model (AOM) parameters provide more chemical insight and will be used to interpret the electronic spectrum.[11] The $\pi$-interaction of the carboxylate oxygen with the metal ion was considered to be anisotropic. The anisotropy of metal-ligand $\pi$-interaction can be expressed by $e_\pi$ parameters in two perpendicular directions, denoted $e_{\pi s}$ and $e_{\pi c}$. By rotation of coordinates through the angle $\psi$, the value of $e_{\pi c}$ can be set to zero, and the $\pi$-interaction of the ligand expressed entirely through $e_{\pi s}$. The ligand field analysis was carried out through an optimized fit of experimental to calculated transition energies. Hoggard has described the methods for determining the eigenvalues and eigenfunctions of a $d^3$ ion in a ligand field from any number of coordinated atoms.[12] The full set of 120 single-term antisymmetrized product wavefunctions was employed as a basis. The Hamiltonian function used in the calculation was

$$\hat{H} = \sum_{i<j} \frac{e^2}{r_{ij}} + V_{LF} + \zeta \sum_i l_i \cdot s_i + \alpha_T \sum_i l_i^2 + 2\alpha_T \sum_{i<j} l_i \cdot s_i \quad (1)$$

the terms of which represent, the interelectronic repulsion, ligand field potential, and spin-orbit coupling, respectively with the last two representing the Trees correction.[13] The $\pi$ - interaction of a nitrogen with $sp^3$ hybridization was assumed to be negligible. The parameters varied during the optimization were the interelectronic repulsion parameters $B$, $C$ and the Trees correction parameter $\alpha_T$, the spin-orbit coupling parameter $\zeta$, plus the AOM parameters, $e_{\sigma O}$ and $e_{\pi O}$ for carboxylate-chromium, and $e_{\sigma N}$ for the amine-chromium. These seven parameters were used to fit ten experimental transition energies: the five $^4A_{2g} \rightarrow \{^2E_{2g}, {}^2T_{1g}\}$ components, identified in Table 4 and the average energies of the transitions to the $^2T_{2g}$, $^4T_{2g}$, and $^4T_{1g}$ gstates. Eigenvalues were assigned to states within the doublet and quartet manifolds based on an analysis of the corresponding eigenfunctions. The function minimized was

$$f = 10^3 S^2 + 10^2 \Sigma D^2 + 10 T^2 + \Sigma Q^2 \quad (2)$$

where $S$ in the first term is the $^2E_g$ splitting, and $D$, $T$, and $Q$ represent the differences between experimental and calculated $\{^2E_g, {}^2T_{1g}\}$, $^2T_{2g}$, and $\{^4T_{2g}, {}^4T_{1g}\}$ transition energies, respectively. The Powell parallel subspace optimization procedure[14] was used to find the global minimum. The optimization was repeated several times with different sets of starting parameters to verify that the same global minimum was found. The results of the optimization and the parameter set used to generate the best-fit energies are also listed in Table 4. The fit is very good for the sharp line

Table 4. Experimental and calculated electronic transition energies for $\Lambda$-*fac*-[Cr(L-ala)$_3$][a]

| State($O_h$) | Exptl | Calcd[b] |
|---|---|---|
| $^2E_g$ | 14378 | 14377 |
| | 14418 | 14418 |
| $^2T_{1g}$ | 15033 | 15001 |
| | 15058 | 15068 |
| | 15106 | 15103 |
| $^2T_{2g}$(avg) | 20665 | 20640 |
| $^4T_{2g}$ | 17760 | 18525 |
| | 19230 | 18840 |
| $^4T_{1g}$ | 24240 | 24670 |
| | 25970 | 25280 |

[a] Data in cm$^{-1}$. [b] $e_{\sigma O}$ = 7747, $e_{\pi O}$ = 1973, $e_{\sigma N}$ = 6432, $B$ = 733, $C$ = 2525, $\alpha_T$ = 228, $\zeta$ = 275.

transitions. The quartet terms were given a very low weight to reflect the very large uncertainty in their position.

The observed $^2E_g$ splitting, 40 cm$^{-1}$ in the excitation spectrum of the title complex is small, compared with the 89 cm$^{-1}$ of *fac*-[Cr(gly)$_3$] (gly = glycine anion).[2] The relative *d*-orbital ordering from the calculations is $xy$ (1883 cm$^{-1}$) < $xz$ (2124 cm$^{-1}$) < $yz$ (2570 cm$^{-1}$) < $x^2$-$y^2$ (20916 cm$^{-1}$) < $z^2$ (20964 cm$^{-1}$). The AOM parameters for L-alanine anion indicate that the carboxylate oxygen is a strong $\sigma$- and $\pi$-donor but is not as strong a $\sigma$-donor as the carboxylate group in the glycine anion. We believe that the slightly weak ligand field properties of L-alanine anion are due to steric effect of extra methyl group. The value of 6432 cm$^{-1}$ for the $e_{\sigma N}$ parameter is a little smaller than the 7505 cm$^{-1}$ reported for [Cr(en)$_3$]Cl$_3$.[15] The cause of the decrease in the value of $e_{\sigma N}$ is presumed to lie in the inductive effect from the adjacent carbonyl group. The AOM parameters could help in determining the geometry of metal complexes with amino acids in the future work. The value of Racah parameter, $B$ is only 79.8 % of the value for a free chromium(III) ion in the gas phase, and we also conclude that electron repulsions are weaker in the complex than the free ion. The ligand field parameters obtained in this study may be transferable to other chromium(III) complexes with this type of amino acids as a basis for schematic analysis.

*Acknowledgement* — Financial support of the Andong National University is gratefully acknowledged.

## REFERENCES


1. Choi, J.-H., I.-H. Suh and S.-H. Kwak (1995) [Bis(3-aminopropyl)amine-*N'*,*N''*,*N'''*][glycylglycinato-*N*,*N'*,*O*]chromium(III) perchlorate monohydrate. *Acta Cryst.* **C51**, 1745-1748.
2. Wallace, W. M. and P. E. Hoggard (1983) Electronic excitation spectroscopy and an angular overlap model analysis of *fac*-tris(glycinato)chromium(III). *Inorg. Chem.* **22**, 491-496.
3. Choi, J.-H. and P. E. Hoggard (1992) Ligand field properties of the peptide nitrogen: The sharp line electronic spectrum of *mer*-di(3-aminopropyl)amine (glycylglycinato-O,N,N' )chromium(III). *Polyhedron* **11**, 2399-2407.
4. Hoggard, P. E (1994) Sharp line electronic spectra and metal ligand geometry. *Top. Curr. Chem.* **171**, 114-141.
5. Choi, J.-H. (1994) Spectroscopic properties and lignad field analysis of tris(*trans*-1,2-cyclohexanediamine) chromium(III) chloride. *Bull. Korean Chem. Soc.* **15**, 145-150.
6. Minor, S. S., G. Witte and G. W. Everett (1976) Cotton effect-configuration relationships in mixed-ligand complexes. 2. The series Cr($\beta$-diketonate)$_n$((S)- amino acidate)$_{3-n}$. *Inorg. Chem.* **15**, 2052-2055.
7. Tsubomura, T., I. Ohkouchi and M. Morita (1991) Luminescence and circularly polarized luminescence of mononuclear and binuclear chromium(III) L-alaninato complexes. *Bull. Chem. Soc. Jpn.* **64**, 2341-2348.
8. Grouchi-Witte, G (1975) Präparative, spektroskopische und chiroptische untersuchungen an L-aninosäure-chrom(III)-komplexen. Dissertation, Universität Hamburg, FRG.
9. Choi, J. -H. (1993) Spectroscopic properties of *cis*-(1,4,8,11-tetraazacyclotetradecane)(1,2-propanediamine) chromium(III). *Bull. Korean Chem. Soc.* **14**, 118-122.
10. Choi, J. -H. and I. -G. Oh (1993) Sharp line electronic spectroscopy and lignad field analysis of *cis*-(1,4,8,11-tetraazacyclotetradecane)(ethylenediamine)chromium (III). *Bull. Korean Chem. Soc.* **14**, 348-352.
11. Choi, J.-H. (1995) A spectroscopic study on the electronic structure of *cis*-[Cr(cyclam)Cl$_2$]Cl. *J. Korean Chem. Soc.* **39**, 501-507.
12. Hoggard, P. E (1986) Sharp line electronic transitions and metal-ligand angular geometry. *Coord. Chem. Rev.* **70**, 85-120.
13. Trees, R. E (1951) Configuration interaction in Mn(II). *Phys. Rev.* **83**, 756-760.
14. Kuester, J. L. and J. H. Mize (1973) *Optimization Techniques with Fortran*, McGraw-Hill, New York, pp.331-343.
15. Choi, J. -H. and T. -H. Lee (1994) Sharp line electronic transitions and metal-ligand geometry of tris (ethylenediamine)chromium(III) chloride. *Korean Appl. Phys.* **7**, 186-192.